Hindawi Publishing Corporation
Journal of Sensors
Volume 2013, Article ID 382726, 7 pages
http://dx.doi.org/10.1155/2013/382726

Research Article

Iron (III) Ion Sensor Based on the Seedless Grown ZnO Nanorods in 3 Dimensions Using Nickel Foam Substrate

Mazhar Ali Abbasi,[1] Zafar Hussain Ibupoto,[1] Yaqoob Khan,[2] Azam Khan,[1] Omer Nur,[1] and Magnus Willander[1]

[1] *Physical Electronics and Nanotechnology Division, Department of Science and Technology (ITN), Campus Norrköping, Linköping University, 60174 Norrköping, Sweden*
[2] *Nanosciences and Catalysis Division, National Centre for Physics, Quaid-i-Azam University Campus, Islamabad 45320, Pakistan*

Correspondence should be addressed to Mazhar Ali Abbasi; mazhar.ali.abbasi@liu.se

Received 19 November 2012; Revised 16 January 2013; Accepted 3 February 2013

Academic Editor: Andrea Cusano

In the present work, the seedless, highly aligned and vertical ZnO nanorods in 3 dimensions (3D) were grown on the nickel foam substrate. The seedless grown ZnO nanorods were characterised by field emission scanning electron microscopy (FESEM), high resolution transmission electron microscopy (HRTEM), and X-ray diffraction (XRD) techniques. The characterised seedless ZnO nanorods in 3D on nickel foam were highly dense, perpendicular to substrate, grown along the (002) crystal plane, and also composed of single crystal. In addition to this, these seedless ZnO nanorods were functionalized with trans-dinitro-dibenzo-18-6 crown ether, a selective iron (III) ion ionophore, along with other components of membrane composition such as polyvinyl chloride (PVC), 2-nitopentylphenyl ether as plasticizer (NPPE), and tetrabutyl ammonium tetraphenylborate (TBATPB) as conductivity increaser. The sensor electrode has shown high linearity with a wide range of detection of iron (III) ion concentrations from 0.005 mM to 100 mM. The low limit of detection of the proposed ion selective electrode was found to be 0.001 mM. The proposed sensor also described high storage stability, selectivity, reproducibility, and repeatability and a quick response time of less than 10 s.

1. Introduction

Iron has remained important for the different biosystems such as haemoglobin, myoglobin, and hem enzymes and also plays role as cofactor in enzyme activities as well as in oxygen transport and electron transport. It has also harmful effects on the various biological systems either in form of being alone or combined state. Due to deficiency of iron anaemia is usually diagnosed, and excess of iron can also be a cause of many health problems. Diseases like cancer, heart problems, and other illnesses such as hemochromatosis are also linked to high level of iron in the body [1–3]. The presence of trace quantity of iron in different substances may result in decay. Several techniques have been used for the detection of iron ion from clinical, medicinal, environmental, and different industrial samples [4–7]. Therefore, it is highly demanded to develop new simple, cheap, fast, and sensitive analytical device for the detection of iron from pharmaceuticals, soil and biological samples. The methods used for the detection of iron are spectrophotometric based on bathophenanthroline, 1, 10-phenanthroline, TPTZ, and ferrozine chemical agents [8–14]. There were few sensors used for the sensing of iron [8, 9] based on the direct potentiometric technique, and it has more advantages than the previously described methods. The membrane ion selective sensor based on coated wire anionic membrane incorporating tetrachloroferrate (III) aliquot has disadvantage of interference with metal cations including Sn2+, Hg2+, and Zn2+ [15]. Beside this, a heterogeneous solid state cationic membrane based on stannic arsenate dispersed in epoxy resin has some problems [16]. The potentiometric sensor was also used in the titration of iron phenanthroline complex against sodium tetraphenylborate solution based on aluminium wire conductor covered with a plasticized PVC membrane [17]. Crown ethers of 18C6 were also employed for

the development of lanthanum [18] and sodium [19] selective electrodes due to their ease in complex formation with metal ions.

Recently, one-dimensional (1D) semiconductor nanomaterials are getting more interest due to their significant contribution in the development of nanoscale-based electronic and optoelectronics devices [20]. Moreover, nanoscale-based materials exhibit distinctive physical and chemical properties. Among them a lot of research is going on the ZnO nanomaterial due to its two prominent properties such as wide band gap (3.37 eV) and high exciton energy (60 meV). Various methods have been used for the synthesis of (1D) ZnO nanostructures including hydrothermal method [21], chemical vapour deposition (CVD) [22], vapor-liquid-solid (VLS) process [23], and template-based methods [24]. The alignment of nanostructures has pronounced effect on the increased working performance of many electronic devices such as short-wavelength lasers [25], gratzel-type solar cell [26], and chemical sensors [27]; therefore more attention is going to the improvement of nanostructures alignment, especially on nanorods and nanowires. The single-crystalline ZnO nanorods have been prepared perpendicularly on sapphire substrates by VLS [23] and CVD techniques [22, 28]. Nevertheless, these techniques follow complicated processes, sophisticated tools, and high temperatures. Many efforts have been taken to control the size and shape of ZnO nanostructures due to the fact that both electronic and optical properties are dependent on the size and dimension [29]. One dimensional nanostructure has remained important for nanophotonic applications such as light emitting diodes, optical waveguides, and nanolasers [30–35] and also to sensor applications including gas sensors [36, 37] and chemical and biosensors [27, 38]. The nanostructures with high surface to volume ratios are more important in the field of sensors and among these nanostructures of ZnO; nanorods are widely used in the fields of chemicals and biosensing due to their high surface to volume ratios [39–44]. The hydrothermal method is becoming more popular among the researchers for the growth of (1D) ZnO nanostructures with peculiar morphologies due to low growth temperature, cheap, fast, simple, dense growth, and ascendible method. Nanostructures have advantage to detect low concentration of analyte from small volumes with high sensitivity.

In this work, seedless ZnO nanorods were grown in 3D on nickel foam substrate. Moreover, trans-dinitro-dibenzo-18-6 crown ether as selective iron (III) ion ionophore was used for the functionalization of seedless grown ZnO nanorods in 3D on nickel foam substrate. The present iron sensor electrode demonstrated good linearity, selectivity, sensitivity, fast response time, and high stability.

2. Materials and Experimental

2.1. Materials. The zinc acetate dihydrate $Zn(CH_3COO)_2 \cdot 2H_2O$, 25% ammonia ($NH_3$), ferric nitrate hexahydrate $(Fe(NO_3)_3 \cdot 6H_2O$, potassium nitrate (KNO_3), tetrahydrofuran (THF), selective iron (III) ionophore trans-dinitrodibenzo-18-6 crown ether, polyvinyl chloride (PVC), 2-nitopentylphenyl ether as plasticizer (NPPE), tetrabutyl ammonium tetraphenylborate (TBATPB) as conductivity increaser were purchased from Sigma Aldrich, Sweden. The nickel foam was purchased from Good fellow Cambridge Limited, England. The nickel foam has thickness and porous size in order (thickness: 1.6 mm, Pores/cm: 20 and with 95% porosity), respectively. All other chemical reagents used were of analytical grade. All the concentrations of analyte were prepared in deionized water.

2.2. The Fabrication of Seedless ZnO Nanorods on Nickel Foam Substrate. The seedless ZnO nanorods were fabricated on nickel foam using zinc acetate dihydrate $[Zn(CH_3COO)_2 \cdot 2H_2O]$ and 25% ammonia aqueous solutions [45]. Prior to the growth process, the nickel foam substrates were sonicated in ultrasonic bath using ethanol solution for 20 minutes, then washed with the deionized water, and dried in air. The dried nickel foam substrates were fixed in Teflon sample holder and kept in mixture of 0.1 M zinc acetate dihydrate and 0.1 M ammonia solutions. Then, the growth solution containing nickel foam substrates was placed in oven at 93°C for 5 to 7 hours. After the completion of growth time, ZnO nanostructures grown nickel foam substrates were washed with the deionized water in order to remove the solid residue particles, and then sample substrates were dried in oven at 80°C for 30 minutes. After this, the seedless grown ZnO nanorods were characterised by field emission scanning electron microscopy (FESEM), high resolution transmission electron microscopy (HRTEM), and X-ray diffraction (XRD).

2.3. Functionalization of Seedless Grown ZnO Nanorods in 3D on Nickel Foam with Selective Iron (III) Ion Ionophore. The seedless grown ZnO nanorods were functionalized with membrane solution consisting of the following composition: 2% trans-dinitro-dibenzo-18-6 crown ether, 63% 2-nitopentylphenyl ether as plasticizer (NPPE), 29% PVC, and 2% tetrabutyl ammonium tetraphenylborate (TBATPB) in 5 mL of THF [46]. The size of working electrode was $2 \times 0.5\ cm^2$. The seedless grown ZnO nanorods based iron sensor electrodes were dipped in this membrane solution for 5 minutes and then dried in air at room temperature for 1 hour. The functionalized electrodes were left in fridge for overnight at 4°C before the experiments.

2.4. Potentiometric Response Measurements. The potential response of the functionalised seedless grown ZnO nanorods in 3D on nickel foam was measured using pH meter model 744 and Keithley 2400 an electrical instrument applied for the measurement of response time of the proposed sensor electrode at 25°C. The cell assembly consisted of two-electrode system; the functionalised seedless grown ZnO nanorods on nickel foam were used as working electrode and the silver/silver chloride (Ag/AgCl) as reference electrode.

3. Results and Discussion

3.1. Characterisation of Seedless Grown ZnO Nanorods in 3D on Nickel Foam. Figures 1(a) and 1(b) referred to FESEM images for the low magnification and high magnification of

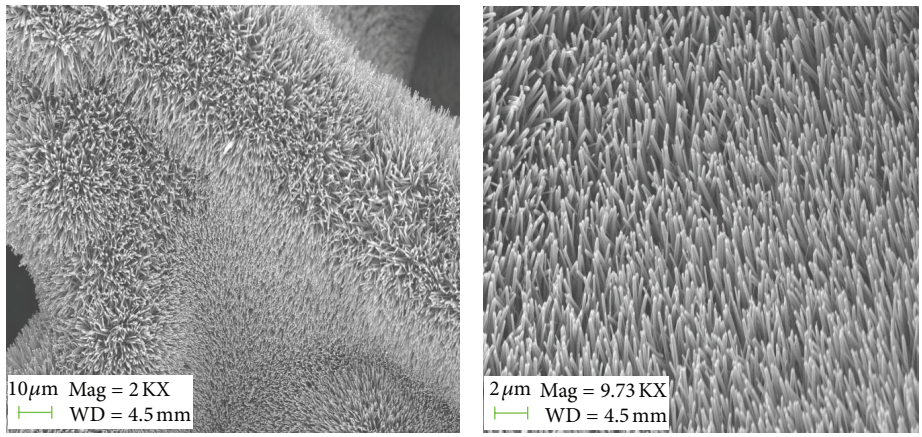

(a) (b)

Figure 1: The (FESEM) images of fabricated ZnO nanorods.

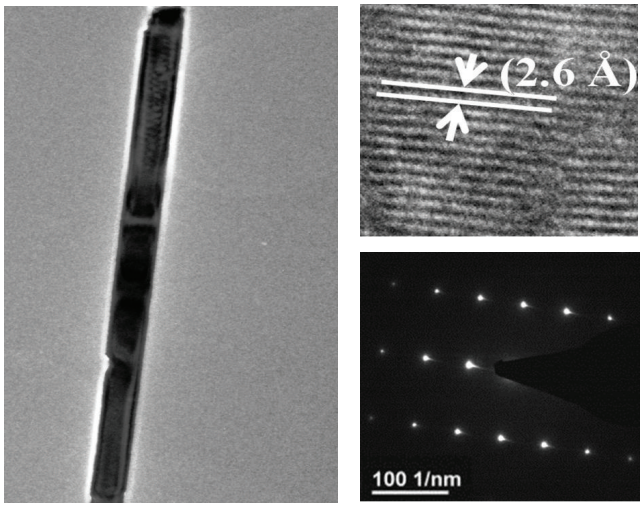

Figure 2: The (HRTEM) images.

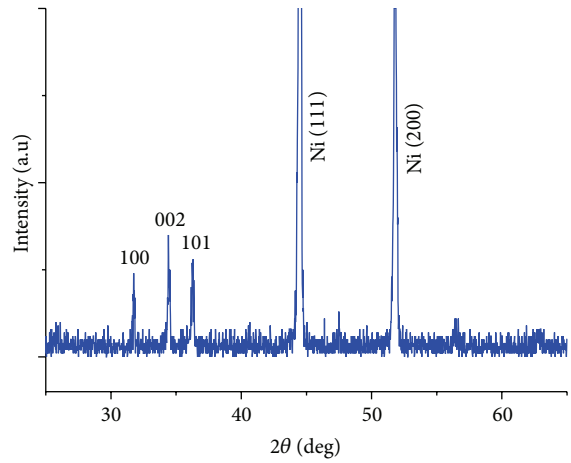

Figure 3: (XRD) analysis of synthesised ZnO nanorods.

seedless grown ZnO nanorods grown on the nickel foam. It can be inferred from Figure 1(a) that for the curved areas of nickel substrate the alignment of the grown ZnO nanorods was changed. But Figure 1(b) shows that the grown ZnO nanorods were highly dense, uniform, vertically aligned, and perpendicular to flat area of the nickel foam substrate. The measured diameter for the seedless grown ZnO nanorods was about 100 nm to 200 nm. The high resolution transmission electron microscopy (HRTEM) of seedless grown ZnO nanorods is shown in Figure 2(a). This study revealed that the grown ZnO nanorods exhibit high crystallinity with lattice spacing of 0.26 nm, which stands for the (002) crystal planes of the crystal lattice of ZnO. In Figure 2(b), a typical selected-area electron diffraction (SAED) pattern is shown for the seedless grown ZnO nanorods. Beside (HRTEM) analysis, the (SAED) observation described that the growth of ZnO nanorods was along the [010] direction and can be listed to the wurtzite structure of ZnO nanorods as shown in Figure 2(c). The XRD study has shown that the appeared peaks were closely related to JCPDS no. 36–1451, and the seedless grown ZnO nanorods exhibited the hexagonal crystalline structure. By comparing with the standard pattern, the (002) plane peak appeared with high intensity than the (100) plane in the present XRD pattern as shown in Figure 3. These obtained results show that the pattern of growth was along the (001) axis.

3.2. Use of Seedless Grown ZnO Nanorods in 3D on the Nickel Foam for the Detection of Iron (III) Ion. The functionalized seedless grown ZnO nanorods based sensor electrode was used for the detection of iron (III) ions from ferric nitrate electrolytic solution. The sensing mechanism of the developed iron ion sensor using ZnO nanorods on nickel foam is described through the schematic diagram as shown in Figure 4. The working electrode consists of the nickel

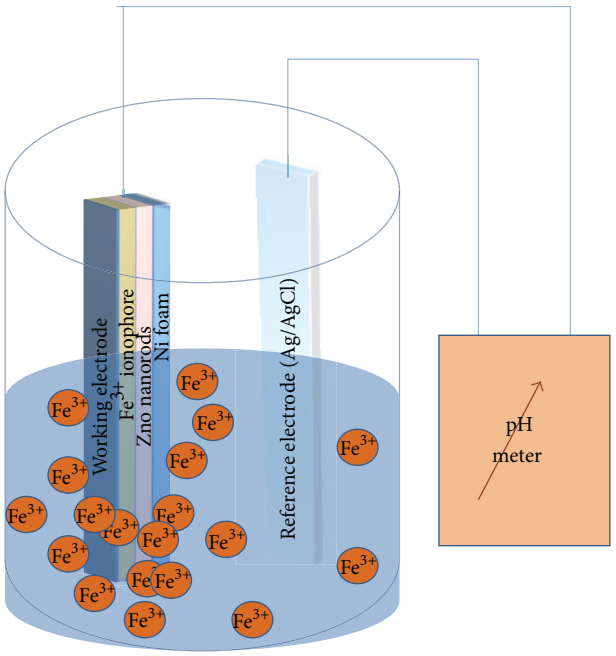

Figure 4: The schematic diagram of the fabricated iron (III) ion sensor.

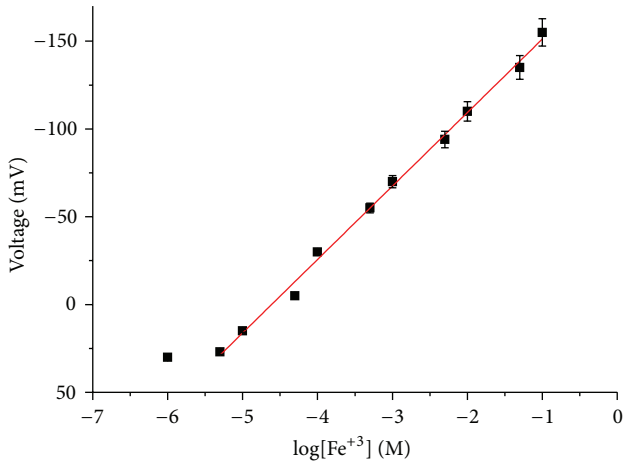

Figure 5: Calibration graph of EMF versus log of iron ion concentrations.

foam, ZnO nanorods and the coating of selective iron (III) ionophore membrane on the nanorods. The ionic strength of analyte solution was adjusted by the use of potassium nitrate. The experimental range of analyte concentrations was selected from 0.001 mM to 100 mM, and all solutions were prepared in the deionized water. The functionalized seedless grown ZnO nanorods on the nickel foam detected the wide range of iron (III) ion concentrations with excellent linearity. The linear range for the present sensor electrode was from 0.005 mM to 100 mM with the sensitivity of 41 mV/decade, and the proposed sensor electrode detected the 0.001 mM concentration of iron ions, but it was beyond the linear range as shown in Figure 5. The high sensitivity and the

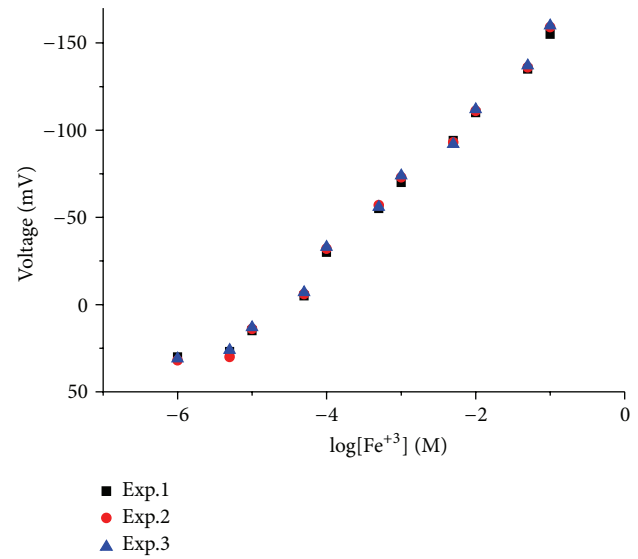

Figure 6: Calibration for repeatability of the proposed iron ion sensor.

wide range detection of iron (III) ion concentrations of the present ion selective electrode could be attributed to the 3D growth of ZnO nanorods on nickel foam which provided maximum surface to the selective iron (III) ionophore for the attachment. Due to this fact rapid complexion was taking place among iron (III) ions and bound iron (III) selective ionophore. Moreover, the nickel foam is porous in nature that helps in the growth of ZnO nanorods in 3D and also provides large surface for the ionophore molecules which further expose higher contact for the capturing of iron ions. Therefore, higher sensitivity and low limit of detection are obtained for the developed iron ion sensor using ZnO nanorods on nickel foam.

3.3. Working Performance of the Proposed Iron (III) Sensor Electrode Based on the Functionalised Seedless Grown ZnO Nanorods in 3D on the Nickel Foam. The repeatability of any of the sensor electrode describes its potential reusability for the certain period of time. In this study, the same ion selective electrode was tested for three consecutive days, and in these three experiments the sensor electrode exhibited almost the same response to the detected range of concentrations as shown in Figure 6.

The reproducibility of the ion selective electrode is important for the observation of a relatively similar response to another electrode prepared under similar set of conditions. In this part of experiment, six independent sensor electrodes were fabricated and functionalised with selective iron (III) ion ionophore and tested into 5 mM electrolytic solution. The sensor electrode revealed good reproducibility with less than 5% standard deviation as shown in Figure 7.

Selectivity of the ion selective electrodes is the back bone parameter for defining their characteristics in the presence of common interferents. It was observed, during the use of the functionalised seedless grown ZnO nanorods based sensor

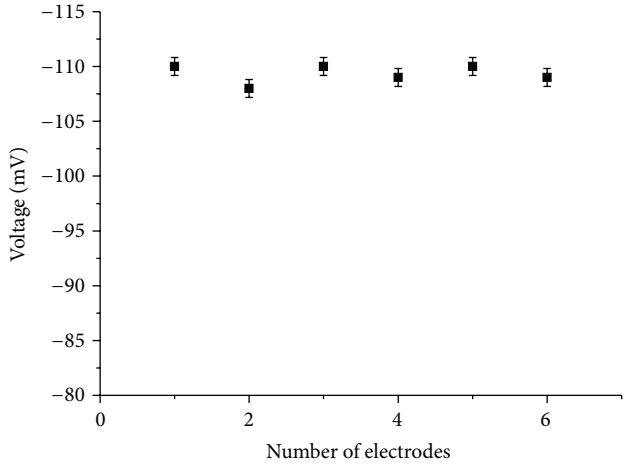

Figure 7: Reproducibility response of different independent iron ion sensor electrodes.

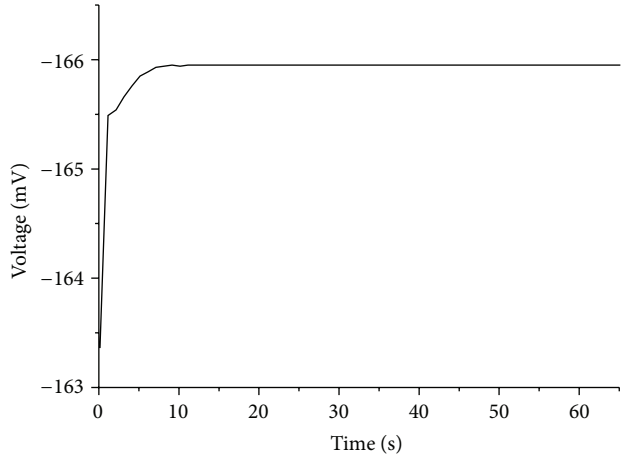

Figure 8: Response time of the present iron ion sensor based on the seedless ZnO nanorods.

electrode into the solutions of different metals, both mono and divalent cation ions such as sodium, potassium, calcium, magnesium, Zinc, nickel, cobalt, silver, and copper ions, that the proposed sensor electrode is highly selective towards iron (III) ions and shows negligible response to these common interferents.

The shelf life of sensor electrode depends on the storage conditions provided for the sensor electrode. Before and after the measurement each sensor electrode was kept at 4°C and used for more than 3 weeks. It was observed that the sensor electrode maintained good storage stability, same sensitivity, and reusability for this period of time.

Besides other characteristics, the proposed iron (III) ion sensor electrode showed the quick output voltage response with respect to time. The proposed iron (III) ion sensor demonstrated a fast response time of 10 s, and the sensor electrode revealed the fast electrochemical signal transfer speed among the highly exposed ZnO nanorods on nickel foam and iron (III) ions in the analyte solution as shown in Figure 8.

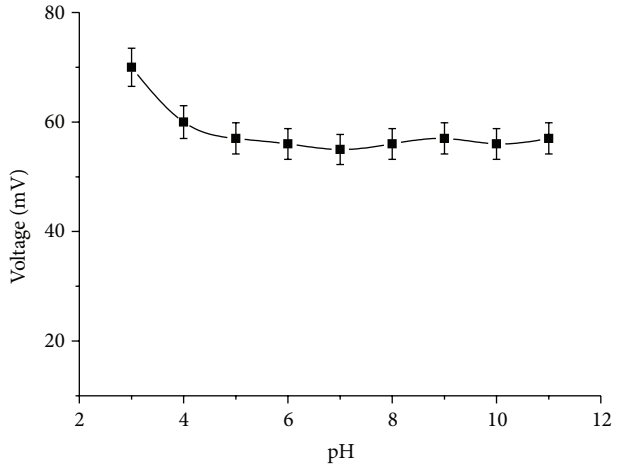

Figure 9: Effect of pH on the output response of proposed iron ion sensor.

3.4. Effect of pH on the Electrochemical Response of Iron Ion Sensor Based on Seedless ZnO Nanorods on Nickel Foam. For describing the working pH range of the present iron ion sensor electrode, a series of pH range was selected from 3–12 as shown in Figure 9. The pH was adjusted by adding 0.1 M hydrochloric acid and sodium hydroxide, respectively. It can be seen that the sensor electrode exhibited almost constant electrochemical response for the wide range of pH values from 5–12, and this describes the potential usability of the sensor for the wide range of pH.

4. Conclusion

In this study, highly perpendicular to substrate seedless ZnO nanorods were grown in 3D on the nickel foam and functionalised with selective iron (III) ion ionophore. The seedless grown ZnO nanorods grown on nickel foam were characterised by FESEM, HRTEM, and XRD techniques. The sensor electrode based on these functionalised seedless grown ZnO nanorods on the nickel foam detected the wide range of iron (III) ions concentrations with good sensitivity of 41 mV/decade and exhibited a fast response time of 10 s. Along these features, the proposed iron (III) ion sensor electrode shows better repeatability, reproducibility, and storage stability. All the obtained results provided the clear evidence for the usability of the present iron ion sensor electrode for the determination of iron ion from the blood samples, clinical, environmental, and other iron containing samples.

Conflict of Interests

The authors do not have any conflict of interests with Sigma Aldrich, Sweden, because this is just a chemicals supplier, and the amount is paid for these chemicals by Linköping university Sweden. Moreover, all authors agreed for the submission of paper.

References

[1] A. F. Oliveira, J. A. Nóbrega, and O. Fatibello-Filho, "Asynchronous merging zones system: spectrophotometric determination of Fe(II) and Fe(III) in pharmaceutical products," *Talanta*, vol. 49, no. 3, pp. 505–510, 1999.

[2] A. Safavi, H. Abdollahi, and M. R. Hormozi-Nezhad, "Simultaneous kinetic determination of Fe(III) and Fe(II) by H-point standard addition method," *Talanta*, vol. 56, no. 4, pp. 699–704, 2002.

[3] R. C. D. C. Costa and A. N. Araújo, "Determination of Fe(III) and total Fe in wines by sequential injection analysis and flame atomic absorption spectrometry," *Analytica Chimica Acta*, vol. 438, no. 1-2, pp. 227–233, 2001.

[4] J. Wu and E. A. Boyle, "Determination of iron in seawater by high-resolution isotope dilution inductively coupled plasma mass spectrometry after $Mg(OH)_2$ coprecipitation," *Analytica Chimica Acta*, vol. 367, no. 1–3, pp. 183–191, 1998.

[5] H. Obata, H. Karatani, and E. Nakayama, "Automated determination of iron in seawater by chelating resin concentration and chemiluminescence detection," *Analytical Chemistry*, vol. 65, no. 11, pp. 1524–1528, 1993.

[6] J. Zolgharnein, H. Abdollahi, D. Jaefarifar, and G. H. Azimi, "Simultaneous determination of Fe(II) and Fe(III) by kinetic spectrophotometric H-point standard addition method," *Talanta*, vol. 57, no. 6, pp. 1067–1073, 2002.

[7] T. Shamspur, I. Sheikhshoaie, and M. H. Mashhadizadeh, "Flame atomic absorption spectroscopy (FAAS) determination of iron(III) after preconcentration on to modified analcime zeolite with 5-((4-nitrophenylazo)-*N*-(2′,4′-dimethoxyphenyl))salicylaldimine by column method," *Journal of Analytical Atomic Spectrometry*, vol. 20, no. 5, pp. 476–478, 2005.

[8] H. Dichl, G. F. Smith, L. McBride, and R. Cryberg, *The Iron Reagents: Bathophenanthroline*, The G. Frederick Smith Chemical Company, Columbus, Ohio, USA, 2nd edition, 1965.

[9] B. G. Stephens and H. A. Suddeth, "Extration of the 1,10-phenanthroline, 4,7-diphenyl-1,10-phenanthroline, and 2,4,6-tripyridyl-sym-triazine complexes of iron(II) into propylene carbonate application to the determination of iron in sea water and aluminum alloy," *Analytical Chemistry*, vol. 39, no. 12, pp. 1478–1480, 1967.

[10] B. G. Stephens and H. A. Suddeth, "Spectrophotometric determination of sulphur dioxide by reduction of iron(III) and simultaneous chelation of the iron(II) with 2,4,6-tri(2-pyridyl)1, 3,5-triazine," *The Analyst*, vol. 95, no. 1126, pp. 70–79, 1970.

[11] M. I. Toral, P. Richter, L. Silva, and A. Salinas, "Determination of mixtures of cobalt and iron by first derivative spectrophotometry," *Microchemical Journal*, vol. 48, no. 2, pp. 221–228, 1993.

[12] L. L. Stookey, "Ferrozine—a new spectrophotometric reagent for iron," *Analytical Chemistry*, vol. 42, no. 7, pp. 779–781, 1970.

[13] Y. Chen, C. M. Ding, T. Z. Zhou, and D. Y. Qi, "Organic solvent-soluble membrane filters for the preconcentration and spectrophotometric determination of iron(II) traces in water with Ferrozine," *Fresenius' Journal of Analytical Chemistry*, vol. 363, no. 1, pp. 119–120, 1999.

[14] B. G. Stephens, H. L. Felkel Jr., and W. M. Spinelli, "Spectrophotometric determination of copper and iron subsequent to the simultaneous extraction of bis(2,9-dimethyl-1,1 ophenanthroline)copper(I) and bis[2,4,6-tri(2-pyridyl)-1,3,5-triazine]iron(II) into propylene carbonate," *Analytical Chemistry*, vol. 46, no. 6, pp. 692–696, 1974.

[15] K. Cammann, *Working With Ion-Selective Electrodes*, Springer, Berlin, Germany, 1979.

[16] D. Ferg, *Ion-Selsctive Electrode Reviews*, vol. 9, Pergamon Press, New York, NY, USA, 1987.

[17] R. W. Cattrall and C. P. Pui, "Coated wire ion selective electrode for the determination of iron(III)," *Analytical Chemistry*, vol. 47, no. 1, pp. 93–95, 1975.

[18] K. Vytras and I. Varmuzova, "Potentiometric ion-pair titrations of metal ions forming complexes with 1,10-phenanthroline and its derivatives," *Electroanalysis*, vol. 6, no. 2, pp. 151–156, 1994.

[19] W. H. Mahmoud, "Iron ion-selective electrodes for direct potentiometry and potentiotitrimetry in pharmaceuticals," *Analytica Chimica Acta*, vol. 436, no. 2, pp. 199–206, 2001.

[20] J. Hu, T. W. Odom, and C. M. Lieber, "Chemistry and physics in one dimension: synthesis and properties of nanowires and nanotubes," *Accounts of Chemical Research*, vol. 32, no. 5, pp. 435–445, 1999.

[21] J. Zhang, L. Sun, H. Pan, C. Liao, and C. Yan, "ZnO nanowires fabricated by a convenient route," *New Journal of Chemistry*, vol. 26, no. 1, pp. 33–34, 2002.

[22] J. J. Wu and S. C. Liu, "Low-temperature growth of well-aligned ZnO nanorods by chemical vapor deposition," *Advanced Materials*, vol. 14, no. 3, pp. 215–218, 2002.

[23] M. H. Huang, Y. Wu, H. Feick, N. Tran, E. Weber, and P. Yang, "Catalytic growth of zinc oxide nanowires by vapor transport," *Advanced Materials*, vol. 13, no. 2, pp. 113–116, 2001.

[24] Y. Li, G. W. Meng, L. D. Zhang, and F. Phillipp, "Ordered semiconductor ZnO nanowire arrays and their photoluminescence properties," *Applied Physics Letters*, vol. 76, no. 15, pp. 2011–2013, 2000.

[25] M. H. Huang, S. Mao, H. Feick et al., "Room-temperature ultraviolet nanowire nanolasers," *Science*, vol. 292, no. 5523, pp. 1897–1899, 2001.

[26] J. Zhong, A. H. Kitai, P. Mascher, and W. Puff, "The influence of processing conditions on point defects and luminescence centers in ZnO," *Journal of the Electrochemical Society*, vol. 140, no. 12, pp. 3644–3649, 1993.

[27] A. Wei, X. W. Sun, J. X. Wang et al., "Enzymatic glucose biosensor based on ZnO nanorod array grown by hydrothermal decomposition," *Applied Physics Letters*, vol. 89, no. 12, Article ID 123902, 3 pages, 2006.

[28] J. J. Wu and S. C. Liu, "Catalyst-free growth and characterization of ZnO nanorods," *Journal of Physical Chemistry B*, vol. 106, no. 37, pp. 9546–9551, 2002.

[29] L. W. Yin, Y. Bando, J. H. Zhan, M. S. Li, and D. Golberg, "Self-assembled highly faceted wurtzite-type ZnS single-crystalline nanotubes with hexagonal cross-sections," *Advanced Materials*, vol. 17, no. 16, pp. 1972–1977, 2005.

[30] J. C. Johnson, H. J. Choi, K. P. Knutsen, R. D. Schaller, P. Yang, and R. J. Saykally, "Single gallium nitride nanowire lasers," *Nature Materials*, vol. 1, no. 2, pp. 106–110, 2002.

[31] X. Duan, Y. Huang, R. Agarwal, and C. M. Lieber, "Single-nanowire elecctrically driven lasers," *Nature*, vol. 421, no. 6920, pp. 241–245, 2003.

[32] M. Law, D. J. Sirbuly, J. C. Johnson, J. Goldberger, R. J. Saykally, and P. Yang, "Nanoribbon waveguides for subwavelength photonics integration," *Science*, vol. 305, no. 5688, pp. 1269–1273, 2004.

[33] C. J. Barrelet, A. B. Greytak, and C. M. Lieber, "Nanowire photonic circuit elements," *Nano Letters*, vol. 4, no. 10, pp. 1981–1985, 2004.

[34] A. B. Greytak, C. J. Barrelet, Y. Li, and C. M. Lieber, "Semiconductor nanowire laser and nanowire waveguide electro-optic modulators," *Applied Physics Letters*, vol. 87, no. 15, Article ID 151103, 3 pages, 2005.

[35] M. Willander, L. L. Yang, A. Wadeasa et al., "Zinc oxide nanowires: controlled low temperature growth and some electrochemical and optical nano-devices," *Journal of Materials Chemistry*, vol. 19, no. 7, pp. 1006–1018, 2009.

[36] H. Zhang, J. Wu, C. Zhai, N. Du, X. Ma, and D. Yang, "From ZnO nanorods to 3D hollow microhemispheres: solvothermal synthesis, photoluminescence and gas sensor properties," *Nanotechnology*, vol. 18, no. 45, Article ID 455604, 2007.

[37] L. Liao, H. B. Lu, J. C. Li, C. Liu, D. J. Fu, and Y. L. Liu, "The sensitivity of gas sensor based on single ZnO nanowire modulated by helium ion radiation," *Applied Physics Letters*, vol. 91, no. 17, Article ID 173110, 3 pages, 2007.

[38] A. Umar, M. M. Rahman, S. H. Kim, and Y. B. Hahn, "ZnO nanonails: synthesis and their application as glucose biosensor," *Journal of Nanoscience and Nanotechnology*, vol. 8, no. 6, pp. 3216–3221, 2008.

[39] L. C. Tien, P. W. Sadik, D. P. Norton et al., "Hydrogen sensing at room temperature with Pt-coated ZnO thin films and nanorods," *Applied Physics Letters*, vol. 87, no. 22, Article ID 222106, 3 pages, 2005.

[40] T. J. Hsueh, S. J. Chang, C. L. Hsu, Y. R. Lin, and I. C. Chen, "Highly sensitive ZnO nanowire ethanol sensor with Pd adsorption," *Applied Physics Letters*, vol. 91, no. 5, Article ID 053111, 3 pages, 2007.

[41] Z. H. Ibupoto, S. M. U. Ali, C. O. Chey, K. Khun, O. Nur, and M. Willander, "Selective zinc ion detection by functionalized ZnO nanorods with ionophore," *Journal of Applied Physics*, vol. 110, no. 10, Article ID 104702, 6 pages, 2011.

[42] Z. H. Ibupoto, S. M. U. Ali, K. Khun, C. O. Chey, O. Nur, and M. Willander, "ZnO nanorods based enzymatic biosensor for selective determination of penicillin," *Biosensors*, vol. 1, no. 4, pp. 153–163, 2011.

[43] Z. H. Ibupoto, S. M. U. Ali, K. Khun, and M. Willander, "L-ascorbic acid biosensor based on immobilized enzyme on ZnO nanorods," *Journal of Biosensors and Bioelectronics*, vol. 2, no. 3, article 110, 2011.

[44] K. Khun, Z. H. Ibupoto, S. M. U. Ali, C. O. Chey, O. Nur, and M. Willander, "Iron ion sensor based on functionalized ZnO nanorods," *Electroanalysis*, vol. 24, no. 3, pp. 521–528, 2012.

[45] Y. khan, S. T. Hussain, M. A. Abbasi, P. -O. Kall, and F. Söderlind, "On the decoration of 3D nickel foam with single crystal ZnO nanorod arrays and their cathodoluminescence study," *Materials Letters*, vol. 90, pp. 126–130, 2013.

[46] G. Ekmekci, D. Uzun, G. Somer, and S. Kalaycı, "A novel iron(III) selective membrane electrode based on benzo-18-crown-6 crown ether and its applications," *Journal of Membrane Science*, vol. 288, no. 1-2, pp. 36–40, 2007.